Published by

British Journal of Contemporary Research

BEXFORD PUBLISHING

Integrated Derivative Thermogravimetric and Raman Spectroscopic Characterisation of Cassava Cortex–Sorbitol Formulations

Original Research Article | Volume 1 | Issue 6 | 2026 | Article Number: 041

Accepted: 25 October 2026 | Published: 10 November 2026 | ISSN: 2979-8582 (Online)

Crossref : **https://doi.org/10.67693/BJCR-X4TC92X6**

Adeniyi Emmanuel Daodu[1], Ekanem Benedict Agbonko[1]

[1]Department of Mechanical Engineering, University of Calabar, Calabar, Nigeria

AED 0009-0006-1915-284X, **EBA** 0000-0002-4724-6169

Correspondence: Adeniyi Emmanuel Daodu, daoduemmanuel@unical.edu.ng

Abstract

This study revisits cassava cortex–sorbitol materials using six original numerical Raman exports and archived thermal records, with particular attention to spectral reliability and the distinction between thermal mass-loss and calorimetric signals. Untreated cassava cortex (CT100), formulations with 5, 15 and 25 wt.% sorbitol (CT5, CT15 and CT25), and sorbitol alone (SB100) were compared; chemically treated cortex (CTT100) was analysed separately. Each Raman export contained 2,090 intensity measurements between 100 and 4,278 cm^{-1}. A reproducible Savitzky–Golay and prominence-based workflow identified the strongest numerical maxima at 2,550, 2,246, 1,366, 2,444 and 1,218 cm^{-1} for CT100, CT5, CT15, CT25 and SB100, respectively. These positions were confirmed directly from the supplied exports but are not necessarily assignable molecular bands; several high-wavenumber spikes require caution. Historical thermal graphs report features at 440, 400, 465, 410 and 370 °C, respectively. Their numerical correspondence with previously reconstructed derivative traces remains unverified; the historical temperatures are therefore presented as source-recorded observations, not independently validated DTG maxima. The Raman records demonstrate sample-dependent spectral variation, whereas the thermal evidence suggests a non-monotonic ordering of graph-reported features. The novelty lies in a transparent, reproducible reassessment of the original Raman measurements and an explicit evidence audit of their proposed thermal integration, extending an earlier thermal-focused report without implying new experiments or unverified structure–property relationships.

Keywords: Cassava Cortex, Sorbitol, Raman Spectroscopy, Derivative Thermogravimetry, Spectral Preprocessing, Lignocellulosic Formulations

© 2026 The Authors. Published by Bexford Publishing Ltd

1. INTRODUCTION

Cassava (Manihot esculenta Crantz) processing yields a heterogeneous peel residue whose inner cortex differs from the external periderm. Using this agricultural residue in materials development could contribute to resource efficiency, but feedstock variability, residual moisture, processing history and component distribution can all influence performance. The mere incorporation of renewable biomass does not establish biodegradability, lower environmental impact or suitability for a specific engineering application [1–3]. Cassava peel fractions should not be treated as chemically uniform: botanical layer, maturity, drying and comminution can affect the distribution of polysaccharides, lignin, extractives and inorganic constituents. Consequently, differences among spectra may reflect both nominal blend composition and local sampling of heterogeneous particles. Reviews of lignocellulosic Raman spectroscopy emphasise this heterogeneity and the need to distinguish compositional markers from optical background [5,6].

Natural-fibre materials contain overlapping contributions from cellulose, hemicelluloses, lignin and extractives. Their responses to heating and optical excitation cannot be interpreted as though they were chemically pure polymers. Recent reviews emphasise the importance of consistent characterisation, moisture management and durability evaluation before performance claims are generalised [1–3]. The cassava cortex examined here was washed, dried, milled and sieved; consequently, the resulting material should be understood as a processed heterogeneous plant-derived fraction rather than purified cellulose [4]. Complementary structural approaches, including NMR, may resolve chemical environments that overlapping Raman features alone cannot establish [11].

Sorbitol is a hydroxyl-rich polyol that may alter the intermolecular environment, water affinity and processing behaviour of carbohydrate-rich formulations. Depending on composition and preparation, hydrogen-bond interactions and physical mixing can influence molecular mobility and the distribution of components. Nevertheless, neither the presence of sorbitol nor a shift in a single thermal feature proves chemical crosslinking, polymerisation or a mechanically effective composite interface. This distinction is especially important when the source preparation description refers to curing reagents but does not provide independent confirmation of a cured network [4]. In a polyol–polysaccharide system, multiple hydroxyl groups offer plausible hydrogen-bonding sites; however, the existence, direction and magnitude of any rearrangement cannot be inferred from nominal sorbitol loading alone. Confirmation would require well-resolved bands, replicate measurements and independent moisture or structural evidence. This distinction is important when interpreting the non-monotonic response of the present specimens.

Raman spectroscopy provides local vibrational information with limited specimen destruction. It is useful for cellulose-rich materials but susceptible to fluorescence, spatial heterogeneity, orientation effects and spectral preprocessing. Agarwal's review describes characteristic cellulose and lignocellulose Raman responses, while the recent study by Agarwal and Ralph demonstrates that xylan can alter bands often treated as cellulose markers [5,6]. Hence, assignments based solely on one strong local maximum are unreliable for complex cassava cortex. The wider biomass Raman literature also demonstrates the value of multiple complementary spectral features and appropriately validated calibration models [6]. Recent overviews of Raman spectroscopy in plant and agricultural research likewise emphasise non-destructive molecular interrogation while recognising sample fluorescence and preprocessing sensitivity [10]. A single dominant algorithmic maximum should therefore not be confused with a chemically identified vibration.

Thermogravimetric analysis measures mass change with temperature; derivative thermogravimetry describes the rate of mass change. In contrast, DSC measures differential heat flow and DTA records temperature difference. These signals cannot be interchanged. A derivative-weight plot alone cannot

© 2026 The Authors. Published by Bexford Publishing Ltd

establish glass-transition temperature, melting enthalpy or the molecular origin of a mass-loss event. Comparisons across formulations also require attention to heating rate, atmosphere, sample mass, baseline and replication [3,4].

The authors' earlier report considered thermal stability and degradation of cassava cortex–sorbitol specimens [7]. The present article addresses a different question: what can be established when the original Raman numerical exports are processed consistently and then evaluated alongside the surviving thermal graphs? Its new contribution is fourfold: (i) direct numerical verification of all six Raman exports, including the treated-cortex comparator; (ii) reproducible extraction of peaks under a common algorithm; (iii) identification of atypical spectral maxima that should not be converted automatically into chemical assignments; and (iv) a documented separation of source-reported thermal features from unverified reconstructed maxima. This approach makes the limits of the archived evidence explicit while establishing a useful foundation for targeted future measurements. Specifically, this work contributes (i) a traceable, uniform reprocessing of six primary Raman text exports; (ii) separate assessment of fingerprint-region responses and conspicuous high-shift numerical maxima; (iii) inclusion of chemically treated cortex as an independent comparator rather than a sorbitol blend; and (iv) a transparent audit of the evidential gap between historical thermal annotations and the unavailable calibrated thermal arrays. Unlike the earlier thermal report, it does not claim a newly measured decomposition temperature or an experimentally established sorbitol-dependent stability optimum.

2. MATERIALS AND METHODS

2.1 Materials and specimen preparation

The underlying M.Eng study reports cassava peel collected in the Akpabuyo area of Cross River State, Nigeria [4]. The outer periderm was removed, and the cortex was washed and rinsed, sun-dried for approximately two weeks until near-constant mass, oven-dried at 50 °C for 24 h, milled and sieved through a nominal 100-mesh (approximately 150 μm) sieve. These details describe the original preparation and were not repeated in the present reanalysis. The project also documents chemical treatment of a separate cortex fraction using alkaline processing and subsequent washing [4]. Because the chemical-treatment sequence introduces additional variables, CTT100 is not included in the untreated sorbitol-dose series.

The source project describes mixing cassava cortex with sorbitol-containing preparations and moulding the mixtures, with nominal sorbitol contents of 5, 15 and 25 wt.% [4]. Its account also mentions methyl ethyl ketone peroxide and cobalt naphthenate, but does not provide independently verified reaction chemistry for the present specimens. The designation "formulation" is therefore retained rather than assuming formation of a chemically crosslinked polymer network.

Specimen	Cassava cortex (wt.%)	Sorbitol (wt.%)	Interpretive role
CT100	100	0	Untreated cortex control
CT5	95	5	Untreated blend
CT15	85	15	Untreated blend
CT25	75	25	Untreated blend
SB100	0	100	Sorbitol control
CTT100	Not part of dose series	Not part of dose series	Chemically treated cortex; Raman only

Table 1. Nominal specimen definitions. Proportions refer to reported formulations rather than independently measured final phase fractions.

© 2026 The Authors. Published by Bexford Publishing Ltd

2.2 Original instrumental measurements

The original project identifies a NETZSCH STA 449C thermogravimetric instrument and reports approximately 8.0 ± 1.5 mg per thermal specimen, heating from 20 to 900 °C at 10 °C min^{-1} under nitrogen (50 mL min^{-1}) [4]. It also describes a separate Q100 heat-flux calorimetric method. Although the project mentions repeated measurements, replicate numerical traces, calibration files and traceable averaging records were not supplied for this reanalysis. Only retained derivative-weight graphs are used here; no calorimetric quantities are reconstructed.

Raman spectra were originally obtained with a Renishaw instrument using 785 nm excitation and a 50× microscope objective; the project gives approximately 25–26 mW laser power [4]. The six supplied text exports each contain 2,090 regularly spaced observations at 2 cm^{-1} intervals, extending from 100 to 4,278 cm^{-1}. Instrument response correction, wavelength calibration records, spatial mapping and repeat spectra are not available in the supplied files.

2.3 Raman numerical processing and evidence classification

Each export was parsed after its acquisition-time and column-header lines. Numerical axis order, step size and finite intensities were checked. Raw signals were smoothed with a Savitzky–Golay filter (window 31 observations; polynomial order three). Local maxima were then detected with a minimum prominence of 35 recorded intensity units and a separation of 15 sampling intervals (30 cm^{-1}). The procedure was applied identically to all six files. Prominence measures the local contrast of a detected feature; it does not prove a Raman vibrational origin [8]. No automatic fluorescence-background removal or cosmic-ray rejection was assumed. Savitzky–Golay smoothing is a local polynomial procedure and can retain broad features while changing narrow spikes, depending on window size [8]. The reported maxima are therefore operational outputs of the specified filter and prominence rule, not invariant molecular peak positions. Instrumental cosmic-ray removal, baseline treatment and independent repeat acquisitions were not documented sufficiently to validate every feature.

For visualisation, median-centred spectra and a separately scaled 350–1800 cm^{-1} fingerprint view were prepared. Scaling is used solely to compare shapes and does not establish concentration or quantitative chemical normalisation. A three-level interpretation was adopted: measured intensity features; algorithmically detected maxima; and molecular assignments requiring independent confirmation. The analysis reports the first two, while reserving the third for future validation [5–7,9,10].

2.4 Thermal-data interpretation

Historical temperatures were transcribed as stated in the original graphs and earlier manuscript. They are not automatically the peak locations of reconstructed derivative curves. Without authenticated original thermal numerical exports, the difference between these representations cannot be resolved reliably. The thermal results are therefore treated as approximate, graph-reported feature locations, with no inferred onset temperatures, residue fractions, activation energies or calorimetric transitions.

3. Results and discussion

3.1 Verification of Raman records

All six files contain 2,090 paired observations on the same wavenumber grid. Uniform processing reproduces the previously listed high-prominence numerical maxima. This is an important reproducibility result, but reproducibility of a numerical algorithm applied to one export is not equivalent to experimental reproducibility. In particular, no replicate acquisitions are available for quantifying specimen-to-specimen or spot-to-spot variability. A common grid permits direct comparison of positions, but not of absolute

© 2026 The Authors. Published by Bexford Publishing Ltd

Raman intensities: acquisition focus, collection efficiency, local roughness and fluorescence can alter count levels. Because the six exports represent separate acquisitions without documented independent replicate spectra, no inferential significance testing or composition–intensity regression is justified.

Specimen	Strongest detected maximum (cm^{-1})	Other prominent maxima (cm^{-1})	Principal caution
CT100	2550	2024, 2514, 3006	High-shift peaks need validation
CT5	2246	2768, 1394	High-shift peaks need validation
CT15	1366	1072, 446	Single export; tentative assignment
CT25	2444	2282, 2766, 440	High-shift peaks need validation
SB100	1218	2838, 438, 3100	Single export; tentative assignment
CTT100	494	180, 2470, 262	Single export; tentative assignment

Table 2. Raman maxima recomputed directly from the supplied original text exports using the stated processing rule.



Figure 1. Savitzky–Golay-smoothed recorded Raman intensities of the five principal formulations. Between-sample absolute intensity is not a calibrated concentration measure.

© 2026 The Authors. Published by Bexford Publishing Ltd

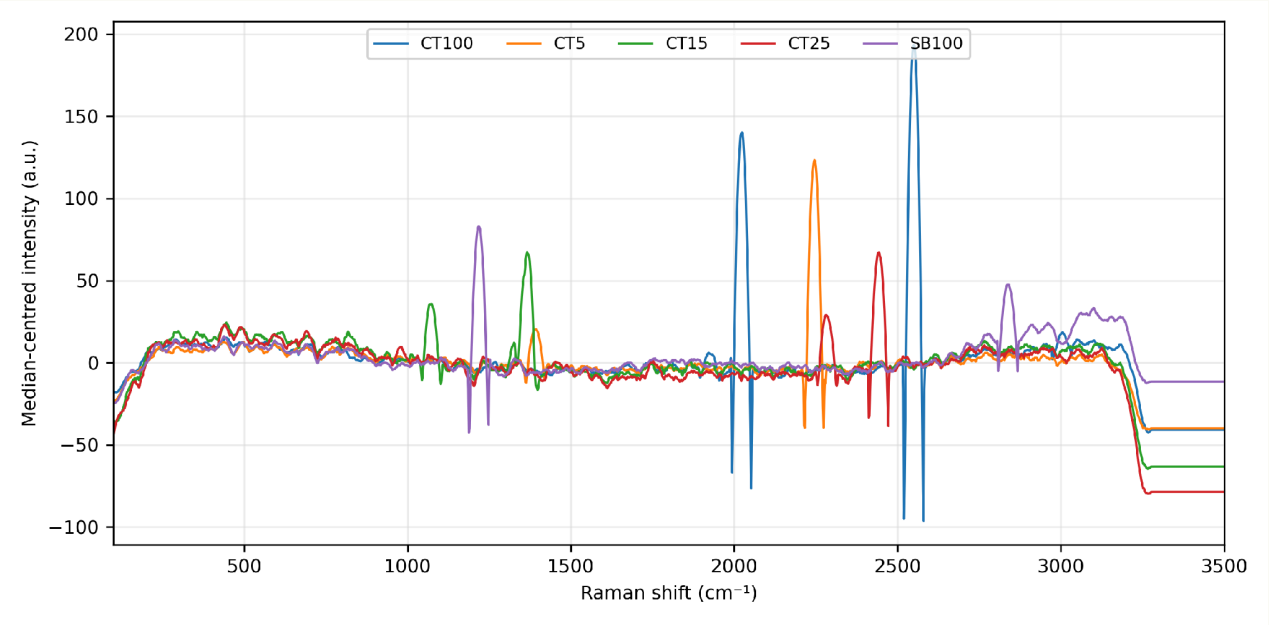


Figure 2. Median-centred Raman responses, presented to show local departures from each specimen's baseline without implying quantitative normalisation.

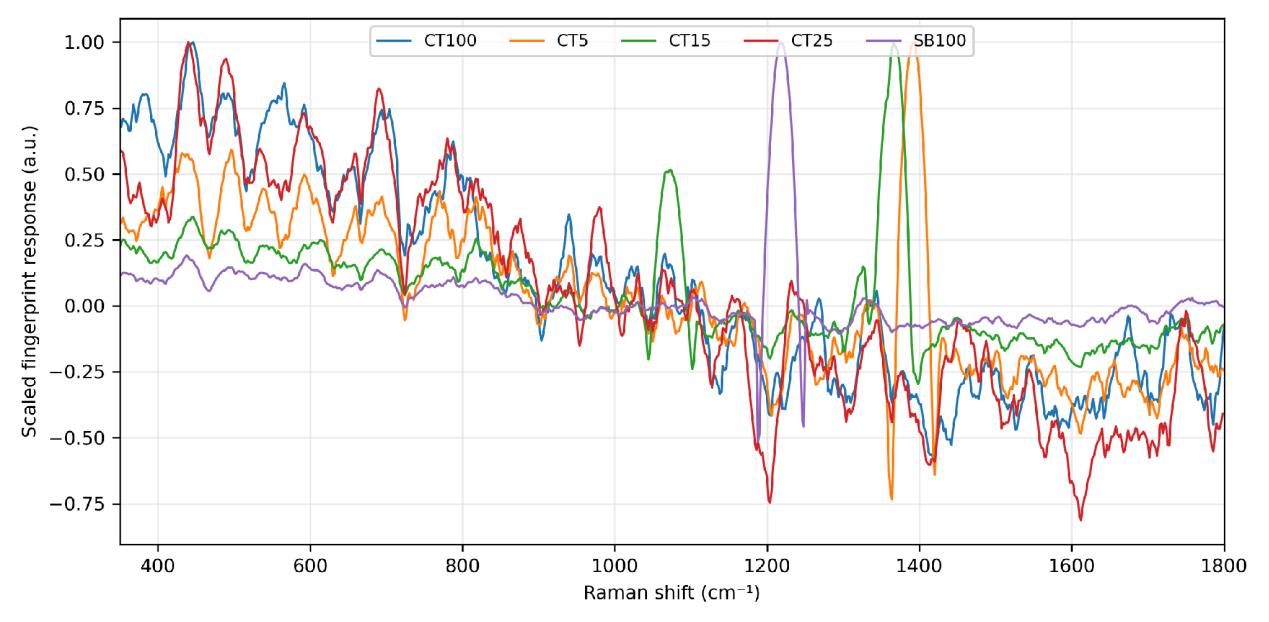


Figure 3. Scaled Raman fingerprint-region comparison (350–1800 cm^{-1}). Scaling is for graphical visibility only; band identities remain provisional.

3.2 Interpretation of constituent controls

CT100 shows the strongest detected maximum at 2,550 cm^{-1}, with other prominent responses at 2,024 and 2,514 cm^{-1}. These are not typical stand-alone diagnostic positions for the cellulose backbone. Their prominence is therefore more appropriately regarded as a warning that local artefacts, optical background or isolated spectral events may dominate the automatic ranking. The fingerprint-region view should receive greater interpretive weight, but even a plausible band requires agreement with reference patterns and repeat measurements [3,5,6]. A high-shift local maximum near 2550 cm^{-1} should not be assigned automatically to cellulose or lignin. It could reflect background structure, an isolated instrumental event, an unrecognised contaminant or a genuine but currently unassigned response. Checking the original

© 2026 The Authors. Published by Bexford Publishing Ltd

unsmoothed neighbourhood and confirming the signal in independent acquisitions would be necessary before chemical attribution. The 2024 investigation of cellulose/xylan Raman spectra underscores the importance of constituent-sensitive, region-specific assignments rather than reliance on global peak ranking [3].

SB100 has its strongest numerical feature at 1,218 cm^{-1}, with further maxima at 2,838 and 438 cm^{-1}. The 2,838 cm^{-1} response falls within a broad region where C–H stretching may occur in organic materials, but an individual maximum is not proof of a unique sorbitol vibration. Sorbitol is retained as the nominal specimen identity supplied by the experimental record; the file label and spectrum alone cannot verify chemical purity.

3.3 Effect of sorbitol fraction on the recorded Raman responses

CT5, CT15 and CT25 do not exhibit a simple progression in the location of their strongest algorithmic peaks. The strongest CT5 response is at 2,246 cm^{-1}, CT15 at 1,366 cm^{-1} and CT25 at 2,444 cm^{-1}. These shifts should not be interpreted as a linear dose response: changing the relative proportions of a heterogeneous biomass and a polyol can alter the sampled microenvironment, but the apparent peak ranking is also sensitive to background and the local intensity distribution. A concentration-dependent assignment would require replicated spectra, defined reference bands, comparable baselines and preferably an independent composition assay [3,5,6]. This absence of a monotonic sequence is scientifically consequential: nominal plasticiser content cannot be used to infer a continuous shift in bonding environment from these spectra. Inhomogeneous mixing, spatially localised sorbitol-rich regions, residual moisture and baseline behaviour offer competing explanations. These are possible mechanisms, not findings demonstrated by the present data.

The CT15 features near 1,072 and 1,366 cm^{-1} lie in spectral regions commonly examined for carbohydrate skeletal and deformation responses. Their positions are consistent with the possibility of overlapping carbohydrate-related vibrations, not definitive evidence of a new bond or a unique cellulose phase. The CT5 feature near 1,394 cm^{-1} similarly cannot establish a specific sorbitol–cortex interaction without corroboration. The present data support the narrower finding that the specimens have distinguishable processed spectral fingerprints. In cellulose-rich materials, the approximately 1000–1500 cm^{-1} interval contains overlapping contributions from carbohydrate skeletal vibrations and CH/CH_2 deformation; assignments can be affected by hemicellulose and lignin [5]. Without spectral deconvolution supported by standards, the features cannot uniquely identify hydrogen-bond rearrangement or quantify the proportion of sorbitol.

3.4 Treated-cortex comparator

CTT100 exhibits strong algorithmic maxima near 494 and 180 cm^{-1}, alongside additional features. Its preparation involved chemical treatment, so its Raman differences cannot be attributed to sorbitol loading. Moreover, the very sharp response around 180 cm^{-1} in the original export warrants particular scrutiny for isolated spikes or optical artefacts before molecular interpretation. CTT100 is reported as contextual evidence from the archive, not included in the five-sample thermal comparison. Chemical treatment may alter extractives, surface chemistry and accessibility, but the treated sample was not part of the CT5–CT25 sorbitol series. It is therefore discussed only as an additional contextual comparison, with no assertion that its numerical peak positions demonstrate treatment efficiency.

© 2026 The Authors. Published by Bexford Publishing Ltd

3.5 Thermal observations and the mismatch between representations

Specimen	Historical graph-reported feature (°C)	Interpretation
CT100	440	Approximate source reading; numerical correspondence unverified
CT5	400	Approximate source reading; numerical correspondence unverified
CT15	465	Approximate source reading; numerical correspondence unverified
CT25	410	Approximate source reading; numerical correspondence unverified
SB100	370	Approximate source reading; numerical correspondence unverified

Table 3. Historical thermal feature temperatures retained from the original experimental record; these are not independently recomputed DTG peak temperatures.

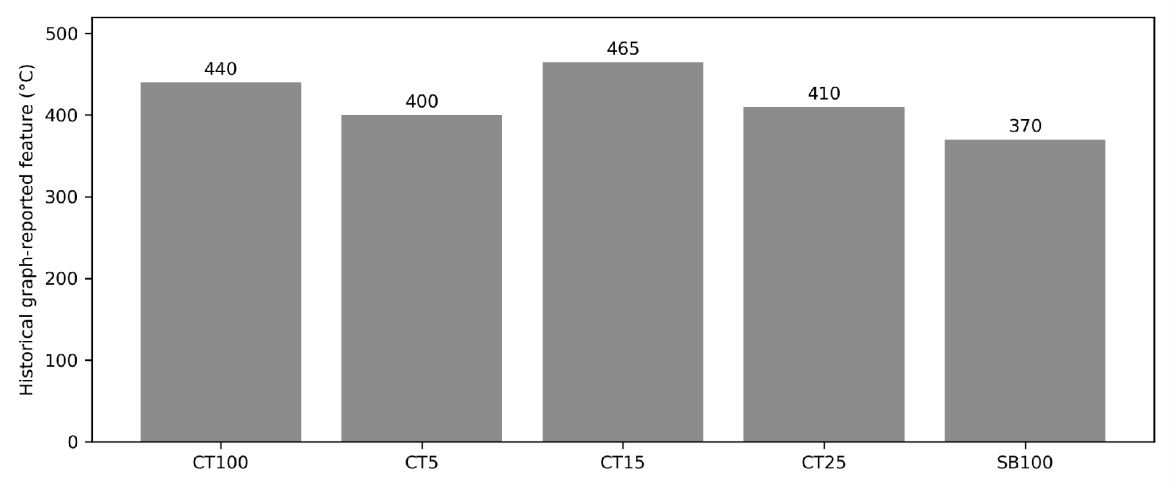


Figure 4. Historical graph-reported thermal feature locations. This is a chart of transcribed values, not a newly reconstructed thermogravimetric trace.

The historical order is CT15 > CT100 > CT25 > CT5 > SB100. If the values correspond to comparable derivative mass-loss events, the non-monotonic pattern would suggest that thermal response is not controlled by sorbitol content alone. Possible contributors include different moisture histories, changes in phase distribution, specimen heterogeneity, multiple overlapping decomposition reactions and sample-to-sample variability. These are plausible mechanisms rather than demonstrated explanations, because the original thermal numerical files and their replicates are not available. Because these are historical annotations rather than re-extracted extrema from authenticated mass-versus-temperature arrays,

© 2026 The Authors. Published by Bexford Publishing Ltd

their ordering must not be interpreted as a statistically established stability ranking. Onset temperature, DTG maximum, residual mass and the atmosphere/heating rate answer different questions and must not be conflated.

The earlier reconstructed derivative-weight curves show prominent troughs at positions that do not agree consistently with the historical values. Replotting those reconstructions while retaining the historical peak list would falsely imply reconciliation. For this reason, this manuscript does not present the disputed curves as authenticated experimental DTG traces. The source values are retained transparently in Table 3 and Figure 4, and the absence of verified thermal exports is stated explicitly. Neither "melting temperature" nor "thermal optimum" is claimed on this basis.

3.6 Integrated scientific implications

Raman spectroscopy probes local molecular polarizability under optical excitation, whereas DTG reflects mass-change kinetics during a temperature programme. Their results are complementary but not causally linked by simple comparison of the strongest Raman wavenumber and a thermal peak temperature. The room-condition Raman spectrum also does not necessarily represent the chemical structure at several hundred degrees Celsius. Establishing such a connection would require matched, replicated measurements, validated baseline treatment, calibrated thermal exports and ideally temperature-resolved spectroscopy or characterisation of heat-treated residues. Raman measurements and mass-loss measurements also interrogate different sample volumes and physical processes; direct mechanistic correspondence requires matched specimens and independently verified events. A plausible change in hydrogen bonding would not by itself establish increased thermal stability, and a shift in an annotated temperature would not prove altered molecular structure.

The contribution beyond the earlier thermal-focused article is therefore methodological and interpretative rather than a new claim of superior material performance. Direct inspection of the six Raman exports confirms the numerical peak rankings and exposes atypical high-shift features; the independent audit of thermal provenance prevents graphical reconstructions from being mistaken for verified instrument peaks. Together, these findings define what can presently be reproduced, what remains tentative and what experiments would resolve the uncertainty.

Evidence	Supported conclusion	Not established
Six numerical Raman exports	Same grid; reproducible algorithmic maxima	Chemical identity or replicate variability
Five untreated formulations	Distinct processed spectral responses	Monotonic sorbitol effect
CTT100 Raman export	Separate treated-cortex fingerprint	Sorbitol-dose effect
Historical thermal graphs	Approximate feature ranking	Authenticated DTG peak temperatures or stability ranking
Cross-method comparison	Complementary observations	Causal spectral–thermal mechanism

Table 4. Evidence boundaries for the integrated interpretation.

© 2026 The Authors. Published by Bexford Publishing Ltd

4. CONCLUSIONS

The six original Raman exports were independently reprocessed with a uniform and explicitly stated algorithm. The principal untreated series shows strongest detected maxima at 2,550 (CT100), 2,246 (CT5), 1,366 (CT15), 2,444 (CT25) and 1,218 cm^{-1} (SB100). These values are reproducible numerical features, but atypical maxima, particularly in the 2,000–2,600 cm^{-1} range, should not be promoted to confirmed chemical assignments without additional controls. The separate treated-cortex spectrum has a distinct response and must not be included in the sorbitol-dose trend. Historical thermal graphs report feature temperatures of 440, 400, 465, 410 and 370 °C in the same principal-sample order; their correspondence with reconstructed derivative traces remains unresolved. The study advances the earlier thermal-focused work by providing a directly reproducible Raman-data analysis and an explicit provenance audit of the proposed thermal integration. Its findings justify further replicated, calibrated and composition-controlled experiments rather than an unsupported claim of optimised thermal performance. The new knowledge is therefore the reproducible description of archived spectral features and the identification of limits on cross-technique inference, rather than a claim that any formulation is definitively optimal. Future confirmation should use replicate Raman acquisitions, fluorescence/background controls, and authenticated TGA/DTG exports recorded under documented atmospheres and heating programmes.

Declarations

Data availability. The six original Raman text exports were supplied for this reanalysis. The original calibrated thermal numerical exports and Raman replicate acquisitions were not available.

Competing interests. The authors declare no known competing interests.

Author contributions. Both authors contributed to interpretation, manuscript preparation and critical revision and accept responsibility for the reported findings.

AI-assisted preparation. AI-assisted tools supported language editing, literature discovery and computational analysis; the authors remain responsible for checking the analyses, sources and final submission.

References

1. Nagaraja S, Anand PB, Kumar MK, Ammarullah MI. Synergistic advances in natural fibre composites: a comprehensive review of the eco-friendly bio-composite development, its characterization and diverse applications. RSC Advances. 2024;14:17594–17611. doi:10.1039/D4RA00149D.

2. Faruk O, Bledzki AK, Fink HP, Sain M. Biocomposites reinforced with natural fibers: 2000–2010. Progress in Polymer Science. 2012;37:1552–1596. doi:10.1016/j.progpolymsci.2012.04.003.

3. Agarwal UP, Ralph SA. Raman spectra of delignified plant fibers: exploring the impact of xylan's presence on the spectral features of cellulose. Fibers. 2024;12(1):5. doi:10.3390/fib12010005.

4. Daodu AE. Thermal characterisation of polymer using natural fibre (cassava cortex) with sorbitol [MEng thesis]. Calabar: University of Cross River State; 2023.

5. Agarwal UP. Analysis of cellulose and lignocellulose materials by Raman spectroscopy: a review of the current status. Molecules. 2019;24(9):1659. doi:10.3390/molecules24091659.

6. Lupoi JS, Gjersing E, Davis MF. Evaluating lignocellulosic biomass, its derivatives, and downstream products with Raman spectroscopy. Frontiers in Bioengineering and Biotechnology. 2015;3:50. doi:10.3389/fbioe.2015.00050.

© 2026 The Authors. Published by Bexford Publishing Ltd

7. Daodu AE, Agbonko EB. Effect of sorbitol content on the thermal stability and degradation behaviour of cassava cortex-reinforced biocomposites. British Journal of Contemporary Research. 2026;1(5):Article 094. doi:10.67693/BJCR-UR74WAGK.

8. Savitzky A, Golay MJE. Smoothing and differentiation of data by simplified least squares procedures. Analytical Chemistry. 1964;36(8):1627–1639. doi:10.1021/ac60214a047.

9. Rinnan Å, van den Berg F, Engelsen SB. Review of the most common pre-processing techniques for near-infrared spectra. TrAC Trends in Analytical Chemistry. 2009;28(10):1201–1222. doi:10.1016/j.trac.2009.07.007.

10. Lemes EM. Raman spectroscopy – a visit to the literature on plant, food, and agricultural studies. Journal of the Science of Food and Agriculture. 2025;105(4):2128–2133. doi:10.1002/jsfa.13803.

11. Parlov Vuković J, Tišma M. The role of NMR spectroscopy in lignocellulosic biomass characterisation: a mini review. Food Chemistry: Molecular Sciences. 2024;9:100219. doi:10.1016/j.fochms.2024.100219.

© 2026 by the authors. Submitted for possible open access publication under the terms and conditions of the **Creative Commons Attribution (CC BY 4.0) licence** (https://creativecommons.org/licenses/by/4.0/)